Mon. Not. R. Astron. Soc. **275**, 685–698 (1995)

A photoionization model of the nebula around the WC11 star M4–18

R. Surendiranath and N. Kameswara Rao
Indian Institute of Astrophysics, Koramangala, Bangalore - 560034, India

Accepted 1995 February 9. Received 1995 January 4; in original form 1994 July 1

ABSTRACT

A photoionization code has been developed incorporating provision for the presence of dust mixed with gas. M4–18 has been modelled utilizing optical CCD spectra and other observations ranging from UV to radio wavelengths. $\bar{T}_e$ and $\bar{N}_e$ from the model are 6600 K and 6050 cm^{-3}, respectively. The abundances of C, N and Ne are found to be the same as the solar values while O is overabundant by a factor of two and S is lower than the solar value by ~90 per cent. A monosized amorphous carbon grain dust model explains the *IRAS* fluxes satisfactorily but emits poorly in the 1- to 10-μm region. M4–18 is a protoplanetary nebula with properties similar to CPD −56° 8032 and V348 Sgr.

Key words: radiative transfer – stars: Wolf–Rayet – dust, extinction – planetary nebulae: individual: M4–18 – infrared: ISM: continuum.

1 INTRODUCTION

M4–18 is a low-excitation planetary nebula, whose central star is a cool Wolf–Rayet star that has been classified as WC10 by Webster & Glass (1974) and later as WC11 by van der Hucht (1981). This rare group of late Wolf–Rayet central stars initially consisted of M4–18, He 2–113, CPD −56° 8032 (hereafter CPD) and V348 Sgr. Their spectra comprise mainly emission lines of He I, C III and numerous lines of C II, in addition to low-excitation nebular lines of [O II], [S II] and [N II]. Lines of [O III] are either absent or weakly present. Large amounts of IR excess radiation is a prominent characteristic of all these objects. Four more objects have been added to this class of WC11 (Cohen & Jones 1987; Menzies & Wolstencroft 1990; Hu & Bibo 1990; Hu & Dong 1992). V348 Sgr, known as a hot RCB star, shows characteristic large light variations while CPD shows small-amplitude light variations. It is not known if others vary in light.

Most of these objects show dust emission features at 7.7, 8.7 and 11.3 μm which are attributed to polycyclic aromatic hydrocarbon (PAH) molecules (Aitken & Roche 1984; Cohen et al. 1986; Cohen & Jones 1987). CO (1–0) and (2–1) emission have been detected in He 2–113, 21282+5050 and CPD (Likkel et al. 1988; Knapp et al. 1989). 07027−7934 has recently been found to show strong 1612-MHz OH maser as well as weak CO emission (Zijlstra et al. 1991).

Rao (1987) compared the nebular and stellar properties of He 2–113, M4–18, CPD and V348 Sgr and indicated the possibility that their evolution might proceed from left to right in the (Log L–Log T) diagram, towards the asymptotic giant branch for a second time and they might form a link with RCB stars. In order to understand the nature of these objects and study their low-excitation nebulae, a photoionization code has been developed and applied to the nebula around M4–18.

The model code is described in Section 2, and the observations are presented in Section 3. The nebular reddening and distance are discussed in Sections 4 and 5. The observational inputs for the central star are analysed in Section 6 and the nebular model is presented and discussed at length in Section 7.

2 THE PHOTOIONIZATION CODE

The model nebula is assumed to be spherically symmetric, static and in steady state. The basic theory is enunciated in Osterbrock (1989). The diffuse radiation field is treated in the OTS approximation. Dielectronic recombination and charge transfer reactions have been included in the ionization equilibrium where appropriate. However, the latter is not considered in the equation for hydrogen for the sake of simplicity. The code provides for inclusion of dust along with gas. The treatment of dust is similar to the approach of Harrington et al. (1988) and Hoare & Clegg (1988). Atomic parameters are taken from the compilation made by Mendoza (1982) and from literature up to 1991. The code has been cross checked for accuracy with results from a known code for a test nebula (Köppen 1991, private communication). A detailed description of the code and atomic parameters are given in Surendiranath (1992).

3 OBSERVATION AND REDUCTION

3.1 Optical and UV spectra

Spectra of M4–18 in the wavelength range ~5500 Å–1 μm were obtained with the 1- and 2.3-m telescopes at the Vainu Bappu Observatory, Kavalur. At the 1-m telescope a Zweiss

Universal Astronomical Grating Spectrograph (UAGS) provided with a Photometrics CCD system containing a Thomson CSF Th7882 chip, was used at the Cassegrain focus with a (2 pixel) resolution of ~14 Å. At the 2.3-m Vainu Bappu Telescope (VBT) a Boller and Chivens spectrograph provided with a CCD camera having a GEC P8603 chip was used and a resolution of 5 Å could be achieved. Table 1 gives the log of observations. The slit was kept N–S in an effort to reduce errors in spectrophotometry due to atmospheric dispersion (Filippenko 1982).

The *International Ultraviolet Explorer* (*IUE*) observations (Figs 1 and 2) were obtained on 1991 August 24, with a large-aperture camera in low-resolution mode covering λ1250–3100 Å.

3.2 Data reduction

All the CCD optical spectra were reduced using the software package RESPECT (Prabhu, Anupama & Giridhar 1987; Prabhu & Anupama 1991). The line equivalent widths were measured by fitting Gaussian profiles and blends were treated as superposed Gaussians. Flux calibration was done by observing the standards He 3 (=EG50) and Feige 34. The fluxes for these are from Barnes & Hayes (1984) and

Table 1. Journal of observations.

Date	Object	Wavelength region Å	Resolution (Å)	Exposure time (Min)	Number of exposures	Sky & seeing
1990 Jan 19/20	M 4–18	5550–7150	14	40	2	Clear sky 2"–2.5"
"	He 3(= EG 50)	"	"	"	1	
1990 Dec 21/22	M 4–18	8300–9950	"	"	4	Fair (cirrus all over) poor seeing.
1991 Feb 10/11	M 4–18	"	15	"	3	Very good ~ 2"
"	Fiege 34	"	"	"	3	
1991 Feb 11/12	M 4–18	7050–8600	"	"	4	Very good ~ 2"
"	Feige 34	"	"	"	3	
1991 Feb 28	M 4–18	5630–6955	5	40	1	Very good 1.2"
1991 Aug 24	M 4–18	LWP 21064 (IUE)	9	100	1	—
"	"	SWP 42313 (IUE)	5	200	1	—
1993 Jan 4/5	M 4–18	9000-10000	4	40	4	Clear sky ~2"

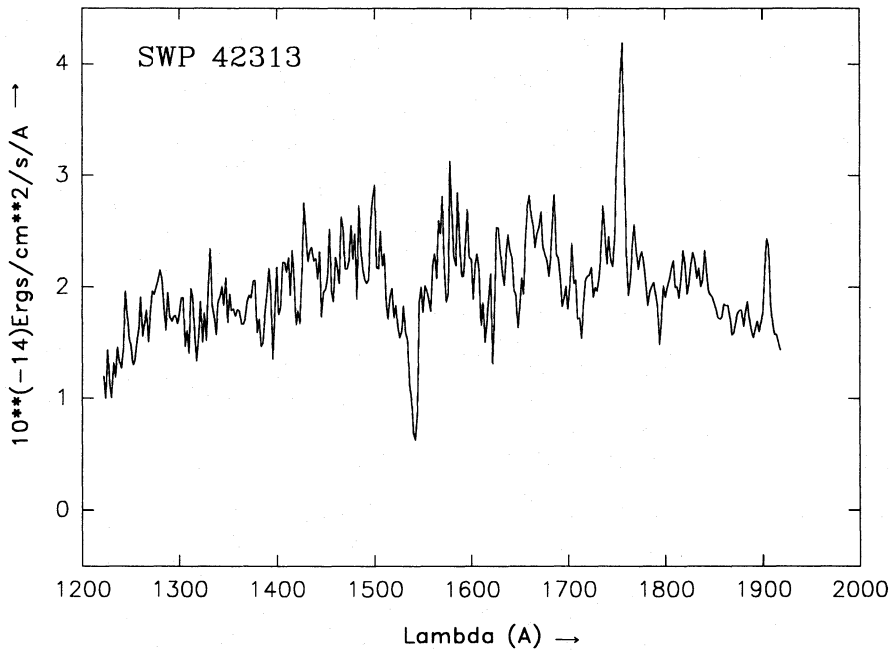

Figure 1. Dereddened *IUE* spectrum (SWP) of M4–18 observed on 1991 August 24, with the large aperture camera in low-resolution mode.

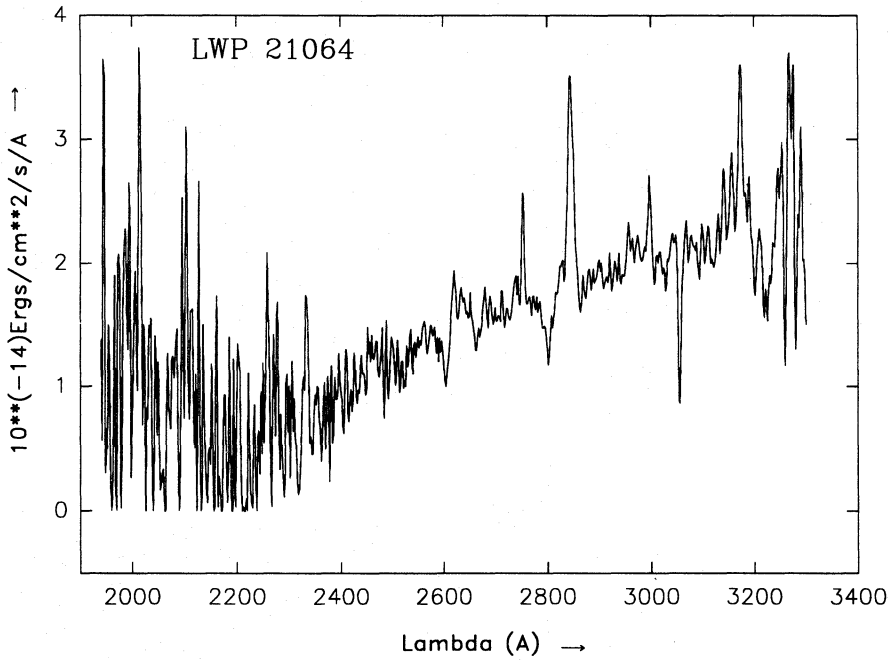

Figure 2. Dereddened *IUE* spectrum (LWP) of M4–18 observed on 1991 August 24, with the large aperture camera in low-resolution mode. +: saturation.

Massey & Gronwall (1990) respectively. Our absolute calibration error is estimated to be a factor of two. The CCD spectra from the 1-m telescope are shown in Fig. 3(a) to (e), and those from the 2.3-m telescope in Fig. 3(f) to (h) and Fig. 4. From a comparison of the measured continuum between our 1-m observations and those of Goodrich & Dahari (1985, hereafter GD) in the wavelength regions common to both, it was noticed that the continuum level of our 1-m spectra was lower; this was more so in the region 7000–9200 Å. GD corrected line fluxes from their red scan in order to make them consistent with the fluxes from their blue and IR scans, and they have ignored small difference between their blue and IR scans. Since no variation of the stellar light has been observed, this continuum level of GD is adopted and extended up to ~7700 Å. The observed V magnitude of Shaw & Kaler (1985) is consistent with this adopted continuum. The line fluxes shown in Table 2 are the product of the measured equivalent width and this adopted continuum. For the region 7700–9000 Å, the lines seen are identified and no fluxes are given due to a poor S/N ratio. In the range 9000 Å–1 μm, our flux calibration is uncertain and the [S III] line (λ9069) flux was calculated by ratioing to the Paschen line (λ9015) for which the flux could be computed. Observations were made with a 2-arcsec slit admitting only a part of the nebula (~4-arcsec diameter) and consequently the absolute fluxes might not represent the whole nebula; however, relative fluxes are expected to be unaltered.

The UV line fluxes from our longer exposure *IUE* spectra are also shown in Table 2. Comparing our measured fluxes with those listed by GD (from archival spectra), our fluxes are lower by a factor of three for C II 1760 Å and C III] 1908 Å, while for C II 2747 Å there is agreement. The line C II 2837.3 Å was completely saturated in our spectrum. We dereddened the measured fluxes using Seaton's (1979) extinction curve.

3.2.1 *Final adopted fluxes*

Our high-resolution spectrum of M4–18 shows a P-Cygni type profile for the lines C II 6462 Å and He I 6678 Å. The measured radial velocities (from the blueshifted absorption dips) are 390 ± 25 and 330 ± 25 km s^{-1} respectively indicating stellar wind. The nebular contribution to the He I line is not easy to separate out. However, in CPD and He 2–113, the H I lines as seen on high-resolution ($\lambda/\Delta\lambda \sim 35\,000$) spectra obtained by one of us (NKR) with the *ESO* 1.5-m telescope, are much sharper relative to C II and He I lines, indicating that H I lines originate from the nebula. For M4–18 we assume that a similar situation prevails and the H I lines are nebular. Some of the nebular lines are blended with the stellar lines e.g. Hβ could have been contaminated by stellar C II (Revised Multiplet Table, 10.01 at $\lambda\lambda$4862, 4867) at our low resolution and the nebular [S II] lines $\lambda\lambda$4068 and 4076 are contaminated (see table 2 of GD) by stellar C II and C III as well as O II lines at $\lambda\lambda$4072 and 4076. Some of the collisional lines used for the nebular diagnostics are unresolved e.g. [O II] $\lambda\lambda$3727, 3729. Although this line was observed by GD, its flux is uncertain because of its proximity to the UV cut-off of the image tube response curve. The [Ne II] λ12.8-μm line flux, as observed by Aitken & Roche (1982, hereafter AR) with a wider aperture which admits the whole nebula, has been included in our analysis.

4 NEBULAR REDDENING AND EXTINCTION

GD used an $E(B-V)$ value of 0.90 ± 0.09 to correct their measured line fluxes for interstellar extinction. It has been pointed out by Rao, Giridhar & Nandy (1990) that the use of 10-GHz radio flux (Purton et al. 1981) and absolute Hβ flux (as given by GD and assumed to be of nebular origin) leads to a value of $E(B-V)$ between 0.41 and 0.56. There-

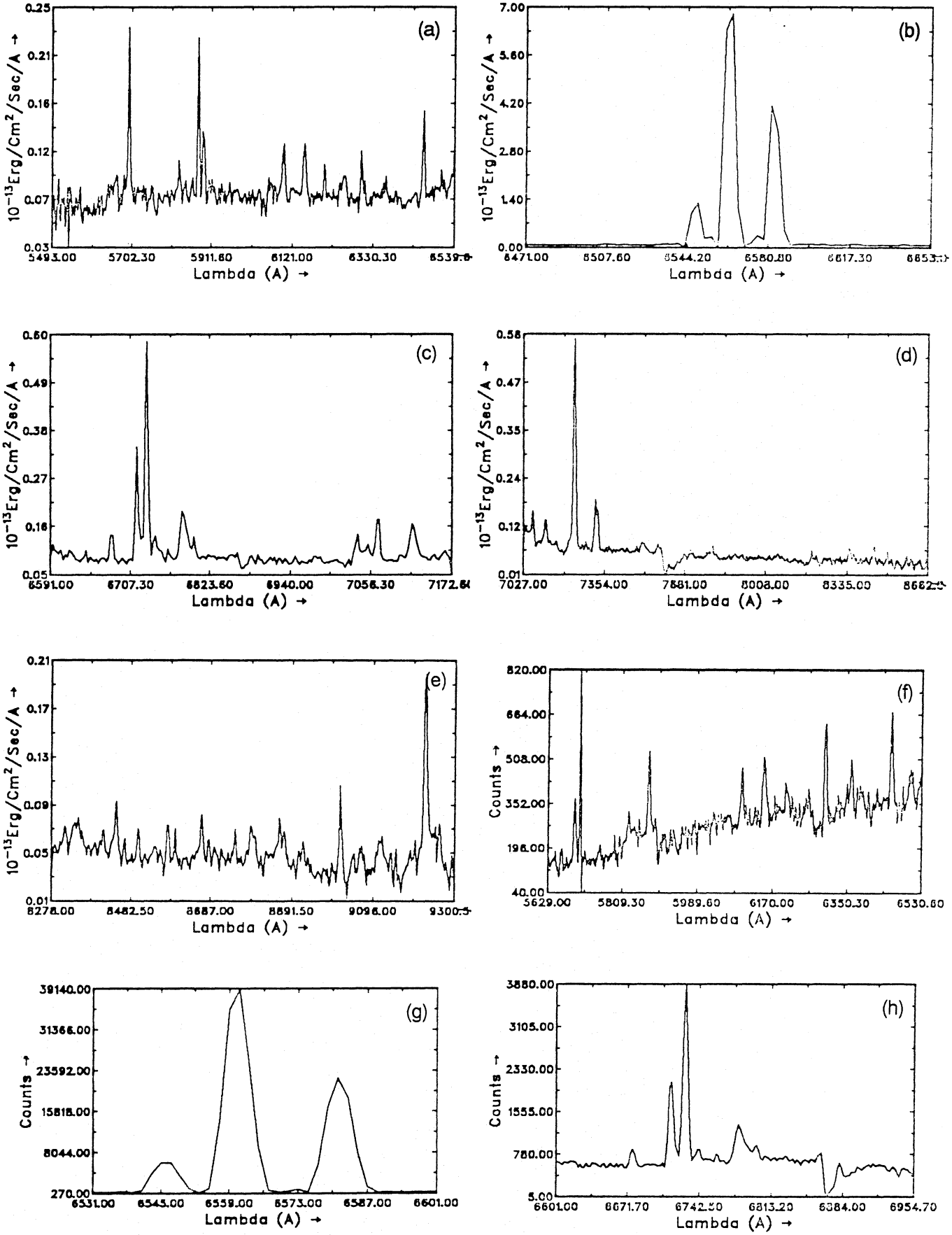

Figure 3. CCD spectra of M4–18 obtained at VBO, Kavalur. (a)–(e) are from UAGS at the 1-m telescope. (f)–(h) are the higher resolution spectra from the B and C spectrograph at the VBT.

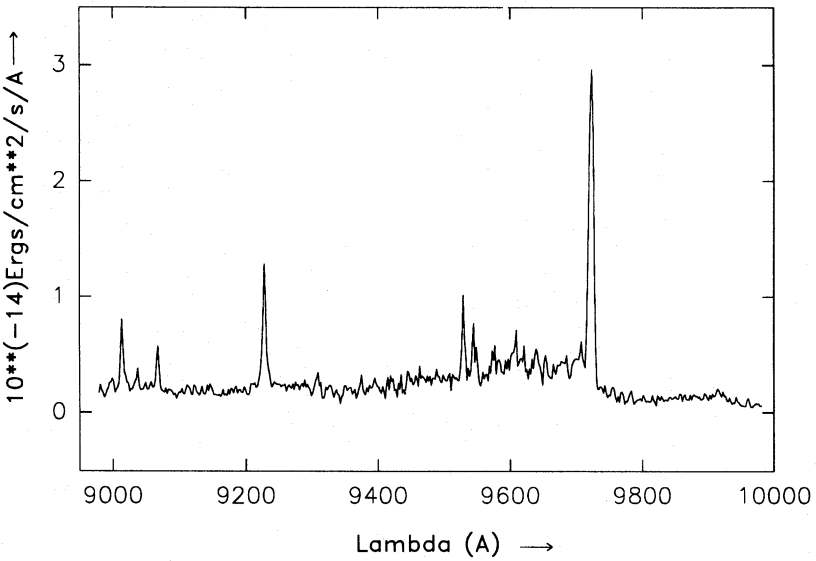

Figure 4. CCD spectrum of M4–18 in the far red (VBT observation).

Table 2. Measured line fluxes.

Measured Wavelength (Å)	Laboratory Wavelength (Å)	Ion	EW(A) New	Measured flux ($10^{-15} ergs\ cm^{-2}\ s^{-1}$) New	Dereddened flux ($10^{-15} ergs\ cm^{-2}\ s^{-1}$) New	GD
1335		C II		13.3	672	
1760		C II		59.3	1860	5800
1908		C III]		40.7	1500	4440
2297		C III		≤6.33	≤329	
2326		C II]		64.7	2870	
2471		[O II]		≤14.7	≤393	
2747		C II		49.3	762	967
2837		C II		Saturated		2770
2993		C II		36.7	434	
3140		?		19.3	204	
3154		?		25.3	265	
3165		C II		80.7	835	
5693.7	5695.9	C III	10.8	102.2	390.3	399.4
	5694.3	C II				
5756.3	5754.6	[N II]	1.30	11.92	44.7	55.2
5826.1	5826.4	C III	1.24	11.1	40.8	54.0
	5823.1	C II				
	5827.8					
5843.7	5843.6	C II	1.47	13.1	47.8	30.6
5862.2	5856.0	C II	1.46	12.9	46.9	46.2
	5863.2	C III				
5877.1	5875.6	He I	11.4	100.4	363.6	338.3
	5876.0					
5889.3	5889.3	C II	6.4	56.3	203.1	225.4
	5889.8					
	5891.6					
6098.9	6095.3	C II	6.3	52.6	179.2	176.4
	6098.5					
	6102.6					
6152.8	6151.4	C II	6.3	52.2	175.2	161.2
6204.6	6205.6	C III	2.8	22.6	74.6	30.8
6244.3	6246.6	C II				
	6250.7					
	6253.8					

Table 2 – *continued*

Measured Wavelength (Å)	Laboratory Wavelength (Å)	Ion	EW(Å)	Measured flux ($10^{-15} ergs\ cm^{-2}\ s^{-1}$)	Dereddened flux ($10^{-15} ergs\ cm^{-2}\ s^{-1}$)	
			New	New	New	GD
6256.3	6256.5	C II				
	6257.2					
	6259.6					
6300.8	6300.3	[O I]	4.1	33.9	109.5	170.9
6307.9			1.3	10.7	34.5	
6332.3						
6362.6	6363.8	[O I]	0.6	5.0	15.9	57.9
6461.5	6462.0	C II	5.4	45.0	139.7	161.4
6507.3			1.36	11.2	34.4	
6549.0	6548.1	[N II]	95.2	786.4	2391.7	2763.3
6563.2	6562.8	H I	587.8	4855.2	14715.5	17024.0
6582.3	6583.6	[N II]	327.3	2703.5	8154.3	8969.0
6593.1			0.53	4.39	13.2	
6617.9			2.4	19.8	59.2	41.0
6641.7			1.0	7.9	23.5	37.5
6679.2	6678.1	He I	4.2	34.3	101.2	124.2
6717.0	6716.4	[S II]	20.2	167.1	489.0	580.0
6731.0	6730.8	[S II]	38.8	319.8	933.1	1132.3
	6727.4	C II				
	6731.0	C III				
6743.0	6742.4	C III	6.2	51.2	148.9	67.2
	6744.4					
6751.5	6750.6	C II	2.9	24.0	69.7	10.7
6763.1	6762.2	C III	2.3	19.0	55.0	41.7
6781.5	6779.9	C II	2.91	24.0	69.2	121.5
	6773.4	C III				
	6774.9					
6785.8	6783.9	C II	12.43	102.7	296.0	228.3
	6787.2					
6793.2	6791.5	C II	1.85	15.3	44.0	102.1
6801.0	6798.1	C II	3.61	29.8	85.6	104.3
	6800.7					
7037.5	7037.2	C III	5.32	43.6	119.2	103.3
7045.4	7046.3	C II	1.23	10.1	27.5	43.2
7052.6	7053.1	C II	3.91	32.0	87.3	56.6
7066.3	7063.7	C II	9.7	80.1	217.7	249.2
	7065.2	He I				
	7065.7					
7100.4			1.3	10.7	28.9	28.6
7113.5	7112.5	C II	7.4	60.7	163.3	
	7113.6					
7116.8	7115.6	C II	2.87	23.5	63.2	
7121.4	7119.9	C II	6.05	49.6	133.3	139.8
	7125.7					
7133.4	7132.4	C II	1.18	9.7	26.0	42.2
	7134.1					
7147.7						
7211.3	7210.5	C III				
	7212.3					
7234.24	7236.4	C II				
	7237.2					
7278.31	7281.3	He I	1.7	14.0	36.4	56.0
7318.0	7318.6	[O II]	18.8	155.2	401.3	371.6
	7319.4					
7328.5	7329.9	[O II]	13.3	109.8	283.4	332.4
	7330.7					
7485.4	7486.5	C III	1.1	9.1	22.8	16.3
7505.3	7505.3	C II				
7506.3	7508.9	C II				

Table 2 – *continued*

Measured Wavelength (Å)	Laboratory Wavelength (Å)	Ion	EW(Å) New	Measured flux ($10^{-15} ergs\ cm^{-2}\ s^{-1}$) New	Dereddened flux ($10^{-15} ergs\ cm^{-2}\ s^{-1}$) New	GD
7525.6	7519.5	C II				
	7519.9					
7704.5	7707.4	C III				
7794.5						
8194.0	8196	[Cl III]?				
8311.2						
8355.0	8357.9	C III				
	8358.7					
8389.7	8392.4	P 20?				
8402.2						
8412.0	8413.4	C II				
	8414.5	C II				
	8412.0	P 19?				
8432.8	8432.8	P 18?				
8445.3		O I				
8466.2	8467.2	P 17?				
8500.9	8500.3	C III				
	8500.9	P 16?				
8542.6	8545.4	P 15?				
8556.5						
8576.7						
8596.2	8598.4	P 14?				
8665.0	8663.6	C III				
8682.8	8682.5	C II				
8696.7	8696.7	C II				
8715.7						
8731.0						
8748.8	8750.5	P 12?				
8787.0						
8796.0	8793.8	C II				
	8799.9					
8851.3						
8860.0	8862.8	P 11?				
8871.8						
8910.0						
8919.1						
9013.1	9014.9	P 10				
9036.9						
9066.5	9068.9	[S III]				
9227.0	9229.0	P 9				
	9229.2	C II				
	9229.8					
9528.8		[S III]				
9544.5		P 8				
9548.6						
9573.0						
9577.2						
9609.0						
9621.1						
9638.5						
9707.0	9701.1	C III				
	9705.4					
	9706.4					
9722.6		C II				

fore an $E(B-V)$ value of 0.48 is adopted in our analysis and the extinction law as given by Seaton (1979) has been used. Shaw (1984) estimates extinction of M4–18 on the basis of detection of Ca II K line in absorption; it could be circumstellar in origin and need not be interstellar. Our value is also consistent with the estimate of $E(B-V)$ of 0.40 by GD using the strong 2175-Å interstellar absorption feature. The dereddened line fluxes are shown in column 6 of Table 2. GD's equivalent widths have been converted to fluxes and dereddened with $E(B-V)$ of 0.48. The dereddened Hβ flux from GD's observations is 5.27×10^{-12} erg cm^{-2} s^{-1}. Shaw & Kaler's (1985) value (from filter photometry) was log $F_{H\beta}=-11.880$. Correcting this with $E(B-V)$ of 0.48 yields an absolute Hβ flux of 6.68×10^{-12} erg cm^{-2} s^{-1}. The mean of these two values (i.e. 5.97×10^{-12} erg cm^{-2} s^{-1}) is adopted for the present analysis.

5 DISTANCE

Nebular mapping with VLA at 5 GHz showed the angular diameter to be 4 arcsec (Zijlstra et al. 1989) which refers to the ionized region. We adopt this as the nebular size although there is a possibility of neutral gas beyond this. With a mean 5-GHz radio flux (mean of Zijlstra et al. 1989 and Aaquist & Kwok 1990) of 20.25 mJy, the distance computed by Daub's (1982) expression is 4.44 kpc. By the modified Shklovskii method the estimated distance is 3.88 kpc; while Cudworth's (1974) scale gives $d=6.47$ kpc, the scale of Mallik & Peimbert (1988) gives $d=7$ kpc. The galactic longitude and latitude of M4–18 are 146° and 7°. Neckel & Klare (1980) give the visual extinction A_V as a function of distance for different galactic longitude and latitude zones. Although the zone of b^{II} around 7° is not covered in their results, it is of interest to estimate the extinction distance from the nearest zone. From their map for the zone 146 + 3° [their Fig. 6b (34)], we get $d=0.63$ kpc. Similarly, the ($E(B-V)$, R, Z) distribution given by Fitzgerald (1968) yields $d=0.65$ kpc [from his fig. 3g (42)] for the the longitude range of 140°–150°, R in the range 100–800 pc and $Z=\pm400$ pc. Pottasch et al. (1984) have shown a clear correlation between nebular radius and dust temperature T_D, where T_D represents the blackbody temperature estimated from *IRAS* fluxes. For M4–18, a blackbody fit of the *IRAS* 12-, 25-, 60- and 100-μm flux densities gives a value of $T_D=230$ K, which is in agreement with 229 K as given by Zhang & Kwok (1990, hereafter ZK). With this T_D, the nebular radius is estimated as $\sim1.6\times10^{16}$ cm (~0.0052 pc). Since the radio angular radius is 2 arcsec, we obtain a distance of 0.6 kpc. Kaler, Mo Jing-Er & Pottasch (1985) have derived an empirical relation that gives distance as a function of stellar luminosity, temperature, visual magnitude and colour excess. This method gives $d=5.63$ kpc for a star assumed to be a blackbody of 23 000 K and radius $r=1.8\times10^{11}$ cm (~2.5 R$_\odot$).

Statistical distances, in general, give very poor estimates when applied to individual nebulae (see Gathier 1984). The extinction distances derived above should also be viewed with caution because extinction varies widely even in directions only 0°.2 away from the object; also, extinction could be very patchy. Since the zone diagrams used in the distance estimates are only neighbourhood representations of the actual direction, there could be an error of a factor of two or three. Therefore a value of 1 kpc has been adopted as a starting value for modelling M4–18; this is also consistent with the estimate from the dust temperature method. With this adopted distance and an angular diameter of 4 arcsec, the outer radius of the nebula is 2.992×10^{16} cm (0.0097 pc).

6 THE CENTRAL STAR

Since the spectrum of the star alone is not available, properties like temperature and radius have to be deduced in other ways.

6.1 Temperature

GD derived a temperature of 22 000 K using the Stoy (1933) energy-balance method, as formulated by Preite-Martinez & Pottasch (1983). By considering the excitation conditions in the nebula as well as that of similar nebular spectra seen in CPD and He 2–113, the above temperature estimate seems to be consistent. The C III/C II line ratio appears to be larger in CPD relative to M4–18. T_* of CPD was estimated to be ~26 000 K by Rao et al. (1990) as well as Aitken et al. (1980). The Zanstra hydrogen temperature for M4–18 is 26 000 K and T_{BB}, by blackbody fit to the dereddened energy distribution in UV and optical, is 23 000 K. Therefore, a value of 23 000 K seems to be appropriate for the central star of M4–18.

6.2 Radius

It has been shown that the core masses of central stars lie in the range 0.546 to ~0.8 M$_\odot$ by Schönberner (1981). Rao (1987) has deduced that the stellar mass is about 0.56 M$_\odot$ for the WC11 group, based on its estimated position in the HR diagram. From its position in the (radio brightness temperature, optical depth at 60 μm) diagram, ZK infer that M4–18 is likely to have a low-mass central star. Assuming that M4–18 represents the minimum mass for a star evolving from AGB to PN we adopt 0.546 M$_\odot$. From the (log L, log T) diagram for a 0.546-M$_\odot$ star (Schönberner & Weidemann 1981) and the above estimate of T_*, an estimate of $R_*\sim2.5$ R$_\odot$ was adopted for M4–18. GD obtained 3.5 R$_\odot$ from the bolometric correction method. Bolometric corrections are not easy to derive for a star whose spectral type and luminosity class are not well defined. However the value of L obtained by the adopted distance, the observed m_v (dereddened), and the bolometric correction (for blackbodies) for $T_*\sim23$ 000 K leads to a much lower luminosity. There is a possibility of neutral extinction occurring around the star, but this has not been taken into account.

6.3 The total energy emitted

The observed UV, optical and IR fluxes (J, H, K and L from ZK, the *IRAS* fluxes from the Point Source Catalogue and the 8- to 13-μm spectrum from AR) along with the radio flux (Purton et al. 1981; Zijlstra et al. 1989; Aaquist and Kwok 1990) in the GHz range are corrected for reddening and plotted in Fig. 5. A blackbody fit for stellar temperature of 23 000 K as well as the 230-K blackbody representing the IR emission by dust are also shown. The observed luminosity of the star (by integration over the range 0.01 to 350 μm) is

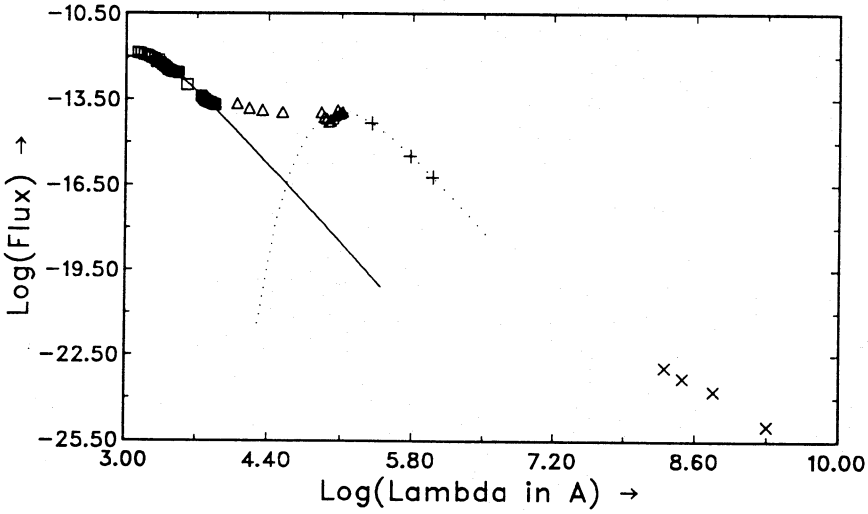

Figure 5. Observed continuum from M4–18. Squares: our new *IUE* and optical observations. Triangles: 8–13 μm spectrum from AR. Plusses: *IRAS* band fluxes. Crosses: VLA observations in the GHz range by Aaquist & Kwok (1990), Purton et al. (1981) and Zijlstra et al. (1989). Solid line: scaled BB (23 000 K) fit. Dotted line: scaled BB (230 K) fit.

164.1 d^2 $L_\odot$, where d is the distance in kpc. The total far-IR luminosity alone is 97.1d^2 $L_\odot$ (after subtracting the 23 000-K scaled BB emission of 67d^2 $L_\odot$) which is about 60 per cent of total flux.

7 THE MODEL

7.1 Physical conditions in the nebula

The diagnostic lines to estimate nebular electron temperature (T_e) and electron density (N_e) are rather limited. The [O III] λ5007 line is not seen in the spectrum. The [N II] λ6584 line is very likely contaminated by stellar C II λ6582 as is the case in CPD. Since our high-resolution spectrum shows that the [N II] lines are well resolved, the observed line flux of [N II] λ6548 was used to compute the expected flux in λ6584. The ratio (I6548 + I6584)/(I5755) gave an estimate of $T_e = 8500$ K from the [log T_e, log N_e] diagram for [N II]. The [O II] line ratios used by GD to estimate T_e may not be reliable, since λ3727 of [O II] is close to the UV cut-off in the response curve of their image tube. The [N II] line ratios of GD are also unreliable because it is uncorrected for blending in λ6584. Kaler (1986) has derived a relation between T_e and the ratio of [C III] λ1908 to C II λ4267. For M4–18, he gives $T_e = 6400 \pm 500$ K using this method. It is likely that the λ1908 line seen in the *IUE* spectrum of M4–18 is of stellar origin, similar to CPD (Rao et al. 1990). We therefore adopt an initial estimate of $T_e = 8500$ K for M4–18.

Although GD state that N_e is well determined from the [S II] line ratio of (I6731/I6717), the line λ6731 is contaminated by stellar C II λ6727.4 and C III λ6731.0. Since it is difficult to quantify the extent of contamination, we avoid using [S II] lines for determining N_e. Therefore, by using Gathier's (1984) expression relating N_e to observed radio continuum flux at 5 GHz, T_e, nebular radius and distance, we derive $N_e = 7600$ cm^{-3}. GD derive $T_e = 5600$ K and $N_e = 1.1 \times 10^4$ cm^{-3} from uncorrected line ratios.

7.2 Nebular abundance

With our derived values of T_e, N_e and line fluxes, abundances of N^+, O^+, O° and S^+ were computed by n-level statistical equilibrium equations. The resulting abundances are [with log $N(H^+) = 12$], log $N(N^+) = 7.6 \pm 0.3$, log $N(O^+) = 8.1 \pm 0.1$, log $N(O^\circ) = 6.9 \pm 0.1$, log $N(S^+) = 6.3 \pm 0.1$ and log $N(S^{++}) = 5.2 \pm 0.1$. For comparison, we recall that in the case of the Sun, log $N(N) = 8.05 \pm 0.04$, log $N(O) = 8.93 \pm 0.04$ and log $N(S) = 7.21 \pm 0.06$. The abundances given by GD [log $N(N^+) = 8.4 \pm 0.3$, log $N(O^+) = 9.7 \pm 0.6$, log $N(O^\circ) = 7.9 \pm 0.4$ and log $N(S^+) = 7.1 \pm 0.3$] are different from our values due to the fact that the electron density and colour excess derived by them are abnormal as shown earlier.

7.3 Dust in the nebula

The dust model, as envisaged in this paper, pertains to the intermixed dust in the ionized region alone. As for the nature of this dust, amorphous carbon grains were considered, since in CPD, Rao et al. (1990) have shown that the feature around 2500 Å could be explained as being due to amorphous carbon. Roche & Aitken (1986) have also suggested that the dust continuum could be due to amorphous carbon in carbon rich PNe. It is likely that the nature of dust particles is similar in all WC11 objects.

The dust modelling formalism adopted in our code follows, in general, the procedure of Harrington et al. (1988), but restricted to monosized grains. Stellar photons and Ly α-line photons were assumed to heat the dust. The mean Q/a values of amorphous carbon (mean of 'BE' and 'XY') from Bussoletti et al. (1987) were used in the wavelength range 2000 Å ≤ λ ≤ 300 μm. For λ < 2000 Å we computed Q_{abs} from the optical constants of Rouleau & Martin (1991), using the Mie theory computer program of Shah (1977).

7.4 Filling factor

The nebula is compact and relatively unevolved; also the VLA 5-GHz contour map indicates a fully-filled nebula. Therefore the filling factor was set at unity (although our code could accommodate fractional values).

7.5 Results

The best matched model parameters are given in Table 3. The mean electron temperature $\bar{T}_e$ and the mean electron density $\bar{N}_e$ are 6600 K and 6050 cm^{-3}, respectively. The ionization structure of H and He are shown in Fig. 6. Fig. 7 shows the same for prominent ions of other elements. Table 4 gives the model and observed line fluxes. The model flux in [S III] λ9069 was matched with observation by reducing sulphur abundance. For the [Ne II] line at 12.8 μm, the agreement between model and observation is good, although we did not change the original abundance which was taken as solar. The model predicts a weak C II] λ2326 line, and the observed flux in this line must be mostly stellar. [O II] λ2471.1 almost agrees with the upper limit derived from our new *IUE* spectra. Within the error limits of observation the agreement between model and observed fluxes is fairly good. The continuum fluxes from UV to far-IR of the model and observation are plotted in Fig. 8. The *B* and *V* fluxes of Shaw & Kaler (1985) are also dereddened and plotted. The nebular abundances are nearly solar (Table 3) except oxygen, which is higher by a factor of two, and sulphur, which is lower by a factor of ~10, compared with the Sun. If we assume that the abundances of N^+, O^+ and S^+ obtained by the line-ratio method represent N, S, and O (since they are mostly present in singly-ionized state throughout the nebula (Fig. 7)), then these are in fairly good agreement with model values but with a large difference in oxygen. When we recalculated the abundances with the model $\bar{T}_e$ of 6600 K, log $N(O^+)$ is 9.03 ± 0.1 for $\bar{N}_e$ = 6050 cm^{-3}, in agreement with the model. We do find an overabundance of oxygen, although not to the extent claimed by GD. As a check we ran a model with T_*, R_* and abundances obtained by GD for a nebula without dust. This model produced $\bar{T}_e$ = 5550 K and $\bar{N}_e$ = 8825 cm^{-3}, close to their quoted value. However, it failed in the following respects: (i) the model stellar luminosity was very high i.e., 2588 $L_\odot$; (ii) the absolute Hβ flux was ~1.5 × 10^2 times what was observed; (iii) the model could not reproduce the observed line fluxes of [O II] 3727 and 3729 Å, and produced very high fluxes in [S III] 9069 and 9532 Å. We ran a model with the same distribution of dust as our model. This also failed in many respects *vis-à-vis* obser-

Table 3. Parameters of the final model for M4–18.

Parameter	Value			
CSPN (BB)				
T_{eff}	22 500 K			
Radius	0.934 $R_\odot$			
Nebula				
Const. density	$N_H = 6\,620\,cm^{-3}$			
Abundance	H	He	C	N
	12.00	10.99	8.56	8.079
	O	Ne	S	Ar
	9.23	8.09	6.00	6.56
Ang. radius	2 arc sec			
Distance	0.9 kpc			
Filling factor	1			
Dust (Amorphous Carbon)				
m_d/m_H	0.1 (inner rad. – 0.0025 r)			
	8.0d–2 (0.0025 r – 0.025 r)			
	5.5d–2 (0.025 r – 0.13 r)			
	2.0d–4 (0.13 r – outer rad.)			
Size distribution	Single size			
Size	0.02 μm			

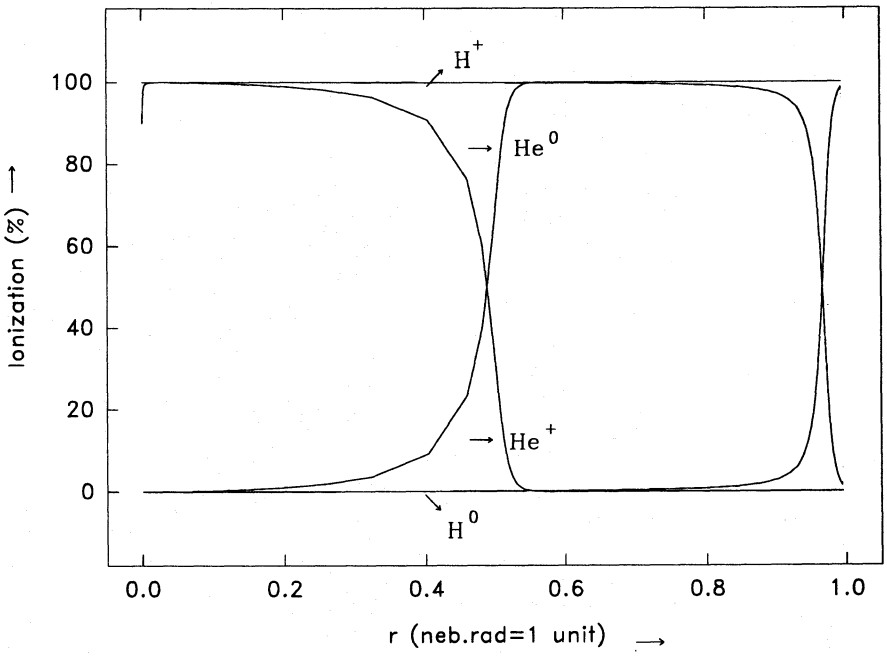

Figure 6. Ionization structure of H and He in M4–18.

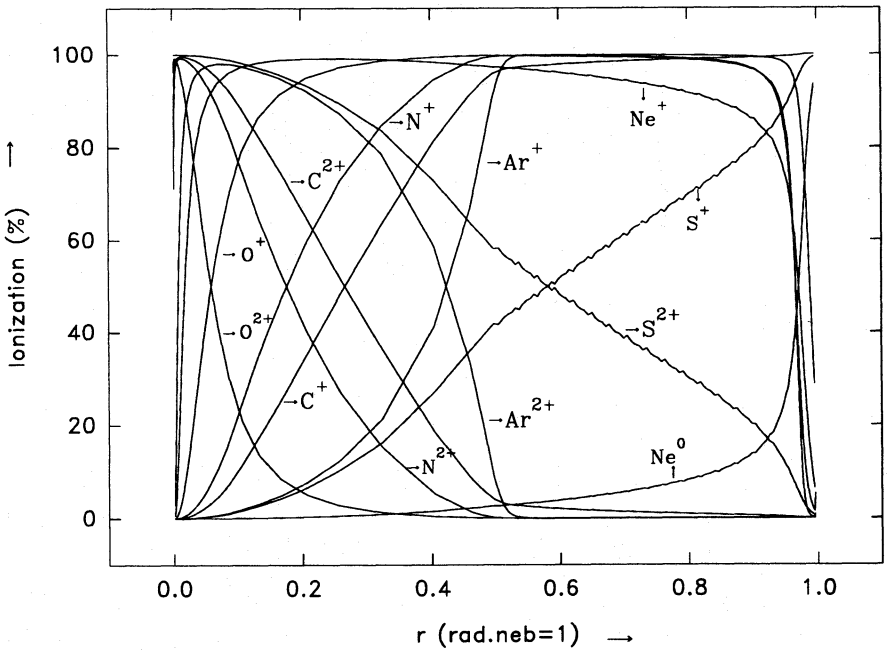

Figure 7. Ionization structure for some of the dominant ions of heavy elements in M4–18.

vations. We checked the sensitivity of our model results for variations in central star temperature, radius and distance of the nebula. The 'spread' in T_*, R_* and d are generally less than ± 200 K, ± 0.1 $R_\odot$ and ± 0.1 kpc respectively.

7.6 Dust radiation

Table 5 gives the model and observed fluxes in the range 1–10 μm and in the *IRAS* bands. The frequencies represent Gaussian abscissae points and the fluxes in the last column are the observed *J*, *H*, *K*, *L* (from ZK) and 10.5-μm (from AR) fluxes given against the closest wavelength of column 1. The model fluxes have been convolved with the system response function of the *IRAS* bands by adopting a procedure similar to Harrington et al. (1988) and the flux densities are compared. Initial models had constant m_d/m_H ratios across the nebula but the resultant IR fluxes did not compare well with observations for various sizes of the grain. We therefore envisaged a step function for the variation of m_d/m_H across the nebula as given in Table 3. The best-fitting grain size was found to be 0.02 μm. Looking at Table 5, it is clear that this model could match the *IRAS* band fluxes satisfactorily, except for the 60-μm band; but emission in the 1–10 μm region is rather low compared with what is observed (see Fig. 9). The model produces 51.5 $L_\odot$ in the IR (1–300 μm) compared with the observed $97.1d^2$ $L_\odot$ (i.e. 78.6 $L_\odot$ for $d = 0.9$ kpc). The deficit of 27.1 $L_\odot$ is not accounted for by the present model. Ly α emission as per the model is 3.34 $L_\odot$. Thus, Ly α makes only a small contribution to the heating of dust. The stellar luminosity from the model is 201.64 $L_\odot$. This is higher than what is observed (132.92 $L_\odot$ for 0.9 kpc). The observed absolute Hβ flux indicates a luminosity of 127 $L_\odot$ for a 22 500 K blackbody. Our model nebula could absorb less than 180 $L_\odot$, leaking out about 21 $L_\odot$. Fig. 10 shows the variation of grain temperature with position. We experimented with larger grains and higher dust temperatures, and found that if the dust temperature at the inner edge of the nebula was allowed to reach ~3000 K, then for a 0.04 μm grain and specific distribution of m_d/m_h along r, we could obtain a satisfactory fit with the observed fluxes in the 1–10 μm region as well as *IRAS* bands. This model had a central star luminosity of about 172 $L_\odot$. It emitted 50 $L_\odot$ in the IR and produced the observed Hβ flux. But grains will sublimate at those high temperatures and will not remain stable. Very small grains (0.005 μm) have a Q_{abs} value (computed using Mie theory) peaking at wavelengths shorter than 912 Å, and this causes skewed absorption by gas and results in insufficient ionization. Our choice of grain size was also guided by the experimental extinction curve (in the region of 500 to 1500 Å) given by Colangeli et al. (1993, see Fig. 2). At around 0.02 to 0.04 μm, our computed Q_{abs} values mimic the trend of the aforementioned experimental curve.

ZK try to explain the IR radiation in M4–18 in terms of a mixture of SiC and graphite. They needed a fraction of 0.21 of SiC and 0.79 of graphite. The feature seen by AR at 11.25 μm was attributed by them to SiC. They also found a 8.65-μm feature and a rise towards a 7.7-μm feature in their spectrum. In their subsequent paper (Roche & Aitken 1986) they suggested that the continuum emission could be due to amorphous carbon grains. On the other hand, ZK attributed the emission in 1–10 μm region as free–free radio continuum. This latter interpretation may not be valid on the ground that the free–free radio emission (extrapolated to the IR region) is two orders of magnitude lower than the observed value. Also, it may be noted that their extracted *IRAS* low-resolution spectrum in the 8–13 μm region is very noisy and has a poorer S/N ratio than the observations of AR.

The present calculations do not take into account effects of scattering, grain growth, destruction etc. A fully-fledged explanation of IR radiation must take into account all of these aspects and modelling with a distribution of grain sizes may have to be explored.

Table 4. Model and observed line fluxes relative to Hα = 100 units.

Ion	Wavelength Å	Model flux ratio	Obsd. flux ratio
C I	8727	0.01	-
»	9823	0.03	-
»	9850	0.10	-
C II	1335	0.30	-
C II]	2326	2.99	≤ 19.5*
C III	2297	0.16	-
[N II]	5755	0.29	0.62
»	6548	18.00	16.20
»	6584	52.99	55.40
[O I]	6300	2.95	0.74
»	6363	0.97	0.11
[O II]	3727	62.74]	93.60
»	3729	24.60]	
»	7321.8	0.50]	2.70
»	7322.4	1.52]	
»	7332.2	0.83]	1.92
»	7332.8	0.82]	
»	2471.0	0.63]	≤ 2.70*
»	2471.1	2.43]	
[O III]	4363	0.00	-
»	4959	0.13	-
»	5007	0.39	-
[Ne II]	128000	22.5	24.40
[S II]	4068	0.18	-
»	4076	0.06	-
»	6717	0.48	3.32
»	6731	0.91	6.34*
[S III]	9069	0.40	0.40
»	9532	0.98	-
»	187000	0.63	-
[Ar III]	7135	0.30	-
		(*Ergs cm^{-2} sec^{-1}*)	
Abs. Hβ flux		5.70d-12	5.97d-12
Abs. Hα flux		1.68d-11	1.47d-11

*Blended with stellar line.

Table 5. Dust radiation in the infrared region.

Wavelength μm	Frequency Hz	Model flux (Ergs/cm^2/sec/Hz)	Obs. flux
1.063	2.8200D+14	1.74D−26	–
1.123	2.6701D+14	2.61D−26	–
1.242	2.4142D+14	5.16D−26	7.92D−25
1.445	2.0752D+14	1.25D−25	–
1.781	1.6831D+14	3.48D−25	1.10D−24[1]
2.355	1.2729D+14	1.06D−24	1.83D−24[2]
3.404	8.8078D+13	3.45D−24	3.96D−24
5.534	5.4177D+13	1.19D−23	–
10.484	2.8594D+13	4.16D−23	2.43D−23
IRAS band fluxes (Jy)			
12	–	6.29	5.21
25	–	8.35	8.97
60	–	7.40	3.49
100	–	1.82	1.97

[1]Flux at 1.65 μm
[2]Flux at 2.20 μm.

7.7 Discussion

7.7.1 Evolutionary status

The luminosity of the model central star is given by $\log(L/L_\odot)=2.30$, which is lower than the luminosity expected from the evolutionary track for 0.545 $M_\odot$ star (Schönberner & Weidemann 1981). Initially, the stellar radius was estimated as 2.5 $R_\odot$ on the basis of the ($\log L$, $\log T_e$) diagram. This gave rise to a much higher luminosity. To achieve agreement with the observed nebular spectrum and dust emission, we require R_* equal to 0.934 $R_\odot$ and d equal to 0.9 kpc. The value for T_{*BB} is consistent with the excitation conditions in the nebula. Even then, the model stellar luminosity of 201.64 $L_\odot$ is higher than the estimated value (132.92 $L_\odot$) for $d=0.9$ kpc. Fig. 8 shows the model continuum (UV and optical) along with what is observed. Assuming uniform expansion, the nebular V_{exp} of 7.5 km s^{-1} (Sabbadin, Bianchini & Hamzaoglu 1984) gives an age of ~1300 yr. Thus, M4–18 is a protoplanetary nebula (PPN). Pollacco et al. (1992) recently discovered photometric variations ($\Delta V=1$) in CPD (compared to a difference of several magnitudes in V348 Sgr). Lawson & Jones (1992) confirmed this from their visual observations and suggest that the general nature of the fade and recovery is similar to the declines of RCB stars. If we consider the angular diameter there is a progression of age from CPD (1.3 arcsec) through M4–18 (4 arcsec) to V348 Sgr (30 arcsec). We find a decrease in the degree of excitation of the emission-line spectrum as we go along the sequence He 2–113, CPD, M4–18 and V348 Sgr, which is indicative of a change in T_{*BB} from higher to lower values. Since CPD exhibits continuum variability (Rao et al. 1990), M4–18 may also show a similar phenomenon. It is not clear in what way these objects differ from other PPN. In a normal PPN, the cooler the star, the more dense (both particle and electron) is the nebula which expands with age. On the other hand, the WC11 group show that objects with cooler central stars have lower N_e (and may be N_H), but larger nebulae.

The dust in M4–18 absorbs more than ~60 per cent of the stellar radiation whereas in the case of CPD it is more than 80 per cent. A proper understanding of the nature, distribution and heating mechanism of dust is essential to fully delineate the nature of the central star. In the case of 07027−7934 the stellar optical flux is ~seven times lower than the IR flux (Menzies & Wolstencroft 1990). At present the nature of these WC11 stars and their relationship to RCB stars is uncertain. M4–18 seems to possess properties intermediate between CPD and V348 Sgr.

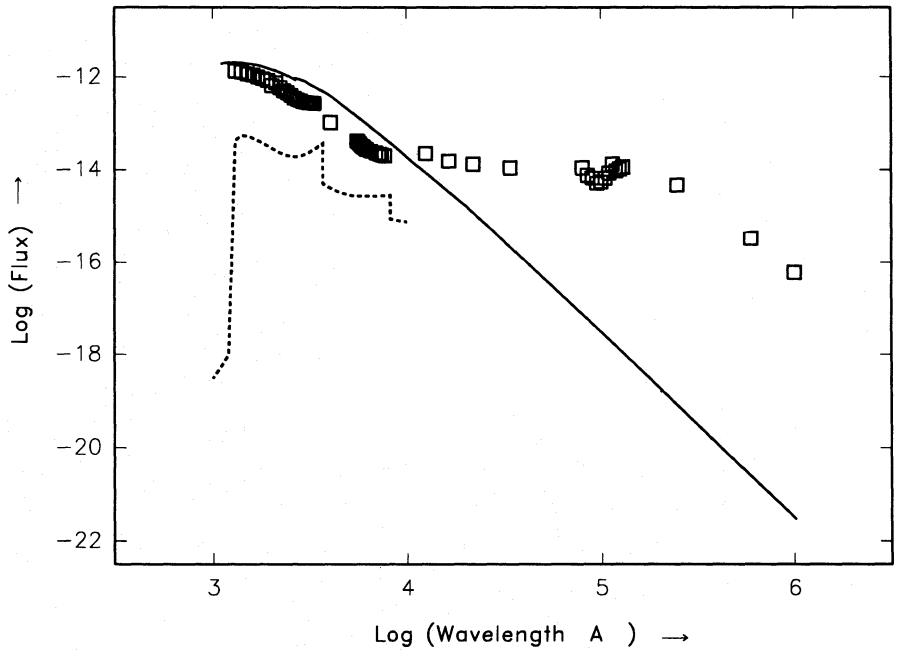

Figure 8. Continuum radiation of model and observation of M4–18. Solid line: stellar continuum. Squares: observed continuum from UV to IR. Dotted line: nebular continuum.

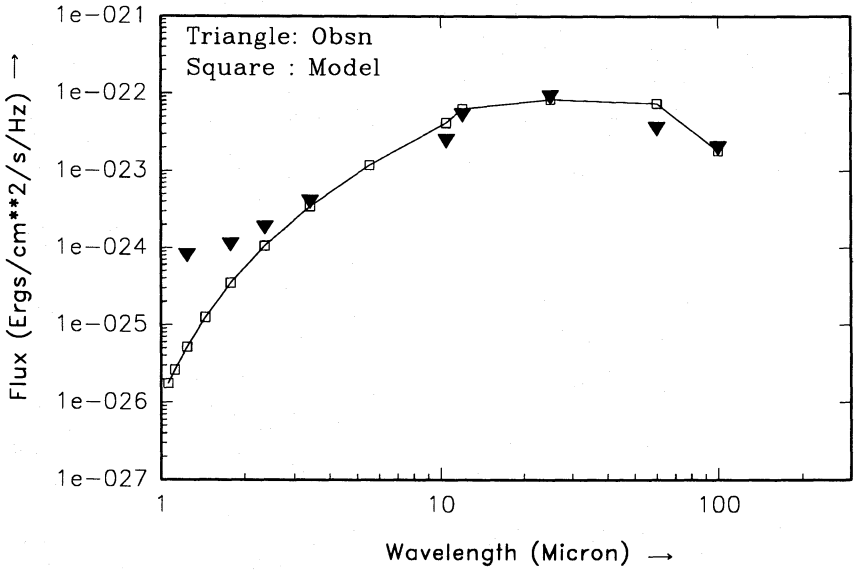

Figure 9. IR fluxes from model and observation.

7.7.2 Conclusions

Our analysis of M4–18 brings out several significant points.

(i) The nebular emission-line spectrum can be well reproduced, with $T_{*BB} = 22\,500$ K, $R_* = 0.934$ $R_\odot$, $d = 0.9$ kpc and a constant density $n_H = 6620$ cm^{-3}.

(ii) For cool central stars, the dust absorbs mostly stellar continuum radiation and Ly α heating is very small. The thermal and ionization structure of the nebula is not drastically affected by well-mixed dust until m_d/m_H is $\sim 10^{-2}$ or higher.

(iii) The dust in M4–18 is likely to be amorphous carbon.

(iv) The properties of M4–18 are similar to CPD and V348 Sgr.

Detailed modelling based on high-resolution spectra and proper treatment of the dust is needed for more WC11 objects to clarify many uncertain aspects.

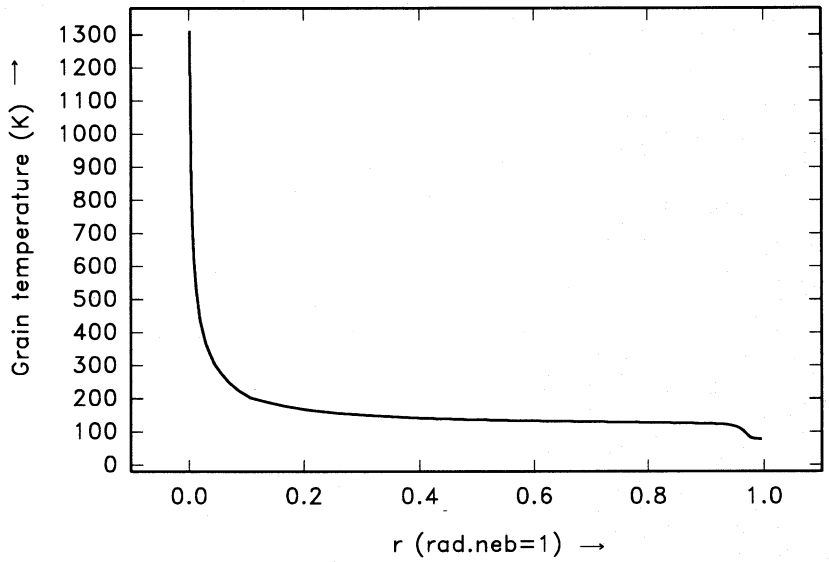

Figure 10. Grain (amorphous carbon, 0.02 μm) temperature shown as a function of position across the nebula.

ACKNOWLEDGMENTS

We thank Dr Joachim Köppen for many helpful suggestions to improve our code and for providing calibration data for checking its accuracy. Dr T. P. Prabhu helped us with CCD spectral reduction. We are thankful to the Director, IIA, for support and the VBO staff for their help during observations. Dr A. Cassatella and Dr J. Fernley along with *IUE* staff at Vilspa are thanked for making the observations for us. One of us (RS) would like to thank Dr D. C. V. Mallik for useful discussions. Finally, we are very grateful to the unknown referee for pointing out the errors in an earlier version of this paper, which resulted in significant revision.

REFERENCES

Aaquist O. B., Kwok S., 1990, A&AS, 84, 229
Aitken D. K., Barlow M. J., Roche P. F., Spenser P. M., 1980, MNRAS, 192, 679
Aitken D. K., Roche P. F., 1982, MNRAS, 200, 217 (AR)
Aitken D. K., Roche P. F., 1984, MNRAS, 208, 751
Barnes J. V., Hayes D. S., 1984, IRS Std. Star Manual (Rev.), KPNO
Bussoletti E., Colangeli L., Borghesi A., Orofino V., 1987, A&AS, 70, 257
Cohen M., Allamandola L., Tielens A. G. G. M., Bregman J., Simpson J. P., Witteborn F. C., Wooden D., Rank D., 1986, ApJ, 302, 737
Cohen M., Jones B. F., 1987, ApJ, 277, 648
Colangeli L., Mennella V., Blanco A., Fonti S., Bussoletti E., Gumlich H. E., Mertins H. C., Jung Ch., 1993, ApJ, 418, 435
Cudworth K. M., 1974, AJ, 79, 1384
Daub C. T., 1982, ApJ, 260, 612
Filippenko A. V., 1982, PASP, 94, 715
Fitzgerald M. P., 1968, AJ, 73, 983
Gathier R., 1984, PhD Thesis, Univ. of Groningen
Goodrich R. W., Dahari O., 1985, ApJ, 289, 342 (GD)
Harrington J. P., Monk D. J., Clegg R. E. S., 1988, MNRAS, 231, 577
Hoare M. G., Clegg R. E. S., 1988, MNRAS, 235, 1049
Hu J. Y., Bibo E. A., 1990, A&A, 234, 435
Hu J. Y., Dong Y. S., 1992, Chin. Sci. Bull., 37, 213
Kaler J. B., Mo Jing-Er, Pottasch S. R., 1985, ApJ, 288, 305
Kaler J. B., 1986, ApJ, 308, 337
Knapp G. R., Sutin B. M., Phillips T. G., et al., 1989, ApJ, 336, 822
Lawson W. A., Jones A. F., 1992, Observatory 112, 1110, 231
Likkel L., Forveille T., Omont A., Morris M., 1988, A&A, 198, L1
Mallik D. C. V., Peimbert M., 1988, Rev. Mex. Astron. Astrofis., 16, 111
Massey P., Gronwall C., 1990, ApJ, 358, 344
Mendoza C., 1982, in Flower D. R., ed., Proc. IAU Symp. 103, Planetary Nebulae. Reidel, Dordrecht, p. 143
Menzies J. W., Wolstencroft R. D., 1990, MNRAS, 247, 177
Neckel Th., Klare G., 1980, A&AS, 42, 251
Osterbrock D. E., 1989, Astrophysics of gaseous nebulae and active galactic nuclei, Univ. Science Books. Mill Valley, CA
Pollacco D. L., Kilkenny D., Marang F., van Wyk F., Roberts G., 1992, MNRAS, 256, 669
Pottasch S. R. et al., 1984, A&A, 138, 10
Prabhu T. P., Anupama G. C., Giridhar S., 1987, Bull. astr. Soc. India, 15, 98
Prabhu T. P., Anupama G. C., 1991, Bull. astr. Soc. India, 19, 97
Preite-Martinez A., Pottasch S. R., 1983, A&A, 126, 31
Purton C. R., Feldman P. A., Marsh K. A., Allen D. A., Wright A. E., 1981, MNRAS, 198, 321
Rao N. K., 1987, QJRAS, 28, 261
Rao N. K., Giridhar S., Nandy K., 1990, A&A, 234, 410
Roche P. F., Aitken D. K., 1986, MNRAS, 221, 63
Rouleau F., Martin P. G., 1991, ApJ, 377, 526
Sabbadin F., Bianchini A., Hamzaoglu E., 1984, A&A, 136, 200
Schönberner D., 1981, A&A, 103, 119
Schönberner D., Weidemann V., 1981, in Iben I. Jr., Renzini A., eds, Physical Processes in Red Giants. Reidel, Dordrecht, p. 463
Seaton M. J., 1979, MNRAS, 187, 73P
Shah G. A., 1977, Kodaikanal Obs. Bull., 2, 42
Shaw R. A., 1984, BAAS, 16, 975
Shaw R. A., Kaler J. B., 1985, ApJ, 295, 537
Stoy R. H., 1933, MNRAS, 93, 588
Surendiranath R., 1992, PhD Thesis, Bangalore University
van der Hucht K. A., Conti P. S., Lundstrom I., Stenholm B., 1981, Space Sci. Rev., 28, 227
Webster B. L., Glass I. S., 1974, MNRAS, 166, 491
Zhang C. Y., Kwok S., 1990, A&A, 237, 479 (ZK)
Zijlstra A. A., Pottasch S. R., Bignell C., 1989, A&AS, 79, 329
Zijlstra A. A., Gaylard M. J., te Lintel Hekkert P., Menzies J., Nyman L.-Å., Schwarz H. E., 1991, A&A, 243, L9